American Society of Hematology
2021 L Street NW, Suite 900,
Washington, DC 20036
Phone: 202-776-0544 | Fax 202-776-0545
editorial@hematology.org

The bone marrow is the primary site of thrombopoiesis

Tracking no: BLD-2023-020895R1

Nathan Asquith (Harvard Medical School, United States) Estelle Carminita (Harvard Medical School, United States) Virginia Camacho (Harvard Medical School, United States) Antonio Rodriguez-Romera (MRC Weatherall Institute of Molecular Medicine, United Kingdom) David Stegner (4. Julius-Maximilians-Universität Würzburg, Rudolf Virchow Center for Integrative and Translational Bioimaging, Germany) Daniela Freire (Harvard Medical School, United States) Isabelle Becker (Harvard Medical School, United States) Kellie Machlus (Harvard Medical School and Boston Children's Hospital, United States) Abdullah Khan (Boston Children's Hospital, United States) Joseph Italiano (Boston Childrens Hospital and Harvard Medical School, United States)

Abstract:
Megakaryocytes generate thousands of platelets over their lifespan. More recently, roles in infection and inflammation have been reported. These findings have driven a study of extra-medullary thrombopoiesis, and megakaryocytes have been increasingly reported within the spleen and lung. However, the relative abundance of megakaryocytes in these organs compared to the bone marrow and the scale of their contribution to the platelet pool in steady state remains controversial. We investigated the relative abundance of megakaryocytes in the adult murine bone marrow, spleen, and lung using whole-mount light sheet and quantitative histological imaging, flow cytometry, intravital imaging, and an assessment of scRNA-seq repositories. Flow cytometry revealed significantly higher numbers of hematopoietic stem and progenitor cells and megakaryocytes in the murine bone marrow compared to spleens or perfused lungs. Two-photon intravital and light-sheet microscopy, as well as cryosections confirmed these findings. Moreover, ex-vivo cultured megakaryocytes from the bone marrow subject to static or microfluidic platelet production assays had a higher capacity for proplatelet-formation than MKs from other organs. Analysis of previously published murine and human scRNA-seq datasets revealed that only a marginal fraction of megakaryocyte-like cells can be found within the lung and most likely only marginally contribute to platelet production in the steady state.

Conflict of interest: COI declared - see note

COI notes: Conflict-of-interest disclosure: J.E.I. has a financial interest in and is a founder of StellularBio, a biotechnology company focused on making donor-independent platelet-like cells at scale. Boston Children's Hospital manages the interests of J.E.I. All other authors declare no competing financial interests.

Preprint server: No;

Author contributions and disclosures: Contribution: N.L.A conducted experiments, analyzed and interpreted the data, and wrote the manuscript; E.C., V.C., D.S., A.A.R., D.F., and I.B. designed and performed experiments and analyzed and interpreted the data. I.B. also critically reviewed the manuscript. K.R.M. provided a critical review of the manuscript. A.K. and J.E.I. conceptualized and designed the research and critically reviewed the manuscript.

Non-author contributions and disclosures: No;

Agreement to Share Publication-Related Data and Data Sharing Statement: Emails to the corresponding author joseph.italiano@childrens.harvard.edu

Clinical trial registration information (if any):

Figure 1

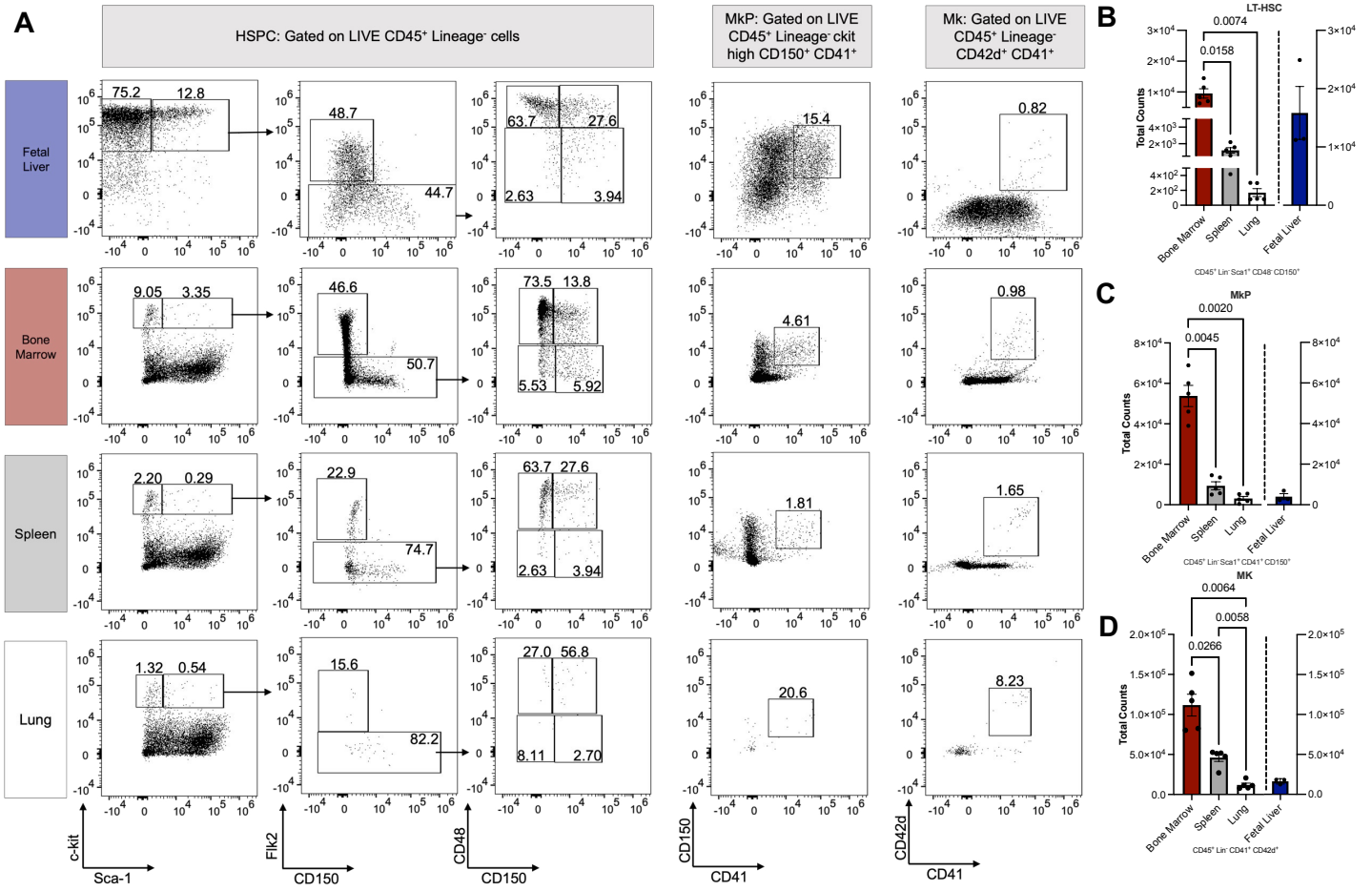
A
HSPC: Gated on LIVE CD45+ Lineage- cells
MkP: Gated on LIVE CD45+ Lineage- ckit high CD150+ CD41+
Mk: Gated on LIVE CD45+ Lineage- CD42d+ CD41+
Fetal Liver
Bone Marrow
Spleen
Lung
75.2
12.8
48.7
44.7
63.7
27.6
2.63
3.94
15.4
0.82
9.05
3.35
46.6
50.7
73.5
13.8
5.53
5.92
4.61
0.98
2.20
0.29
22.9
74.7
63.7
27.6
2.63
3.94
1.81
1.65
1.32
0.54
15.6
82.2
27.0
56.8
8.11
2.70
20.6
8.23
c-kit
Sca-1
Flk2
CD150
CD48
CD150
CD150
CD41
CD42d
CD41
B
LT-HSC
0.0074
0.0158
Total Counts
Bone Marrow
Spleen
Lung
Fetal Liver
C
MkP
0.0020
0.0045
Total Counts
Bone Marrow
Spleen
Lung
Fetal Liver
D
MK
0.0064
0.0058
0.0266
Total Counts
Bone Marrow
Spleen
Lung
Fetal Liver

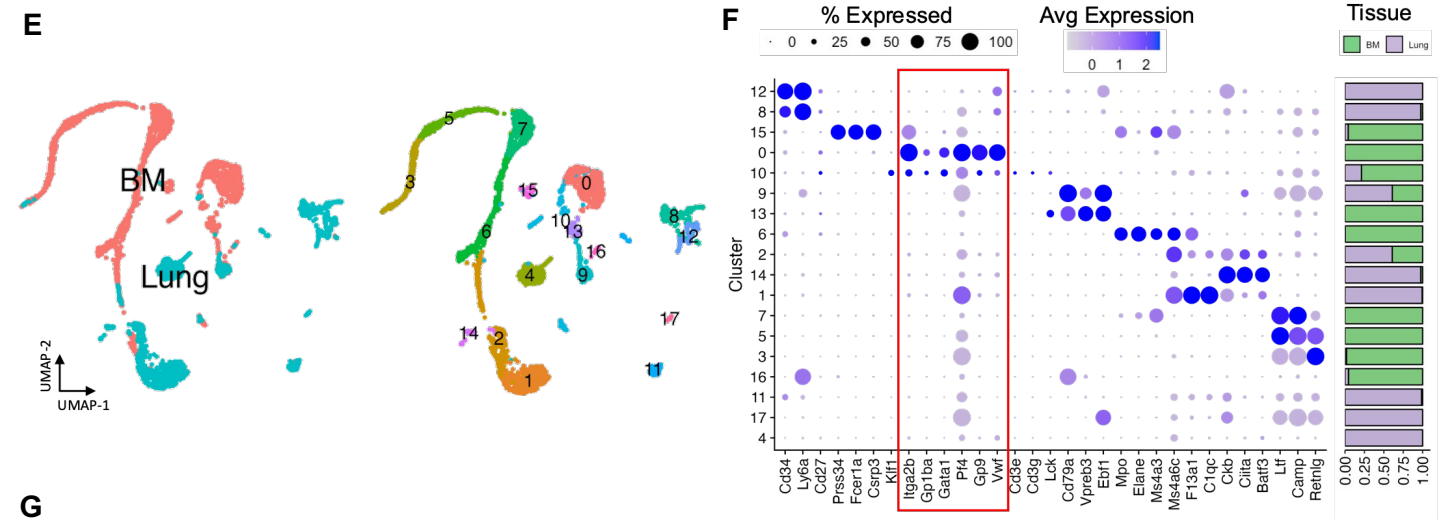
E
BM
Lung
UMAP-2
UMAP-1
F
% Expressed
0 25 50 75 100
Avg Expression
0 1 2
Tissue
BM
Lung
Cluster
Cd34 Ly6a Cd27 Prss34 Fcer1a Csrp3 Klf1 Itga2b Gp1ba Gata1 Pf4 Gp9 Vwf Cd3e Cd3g Lck Cd79a Vpreb3 Ebf1 Mpo Elane Ms4a3 Ms4a6c F13a1 C1qc Ckb Ciita Batf3 Ltf Camp Retnlg
0.00 0.25 0.50 0.75 1.00

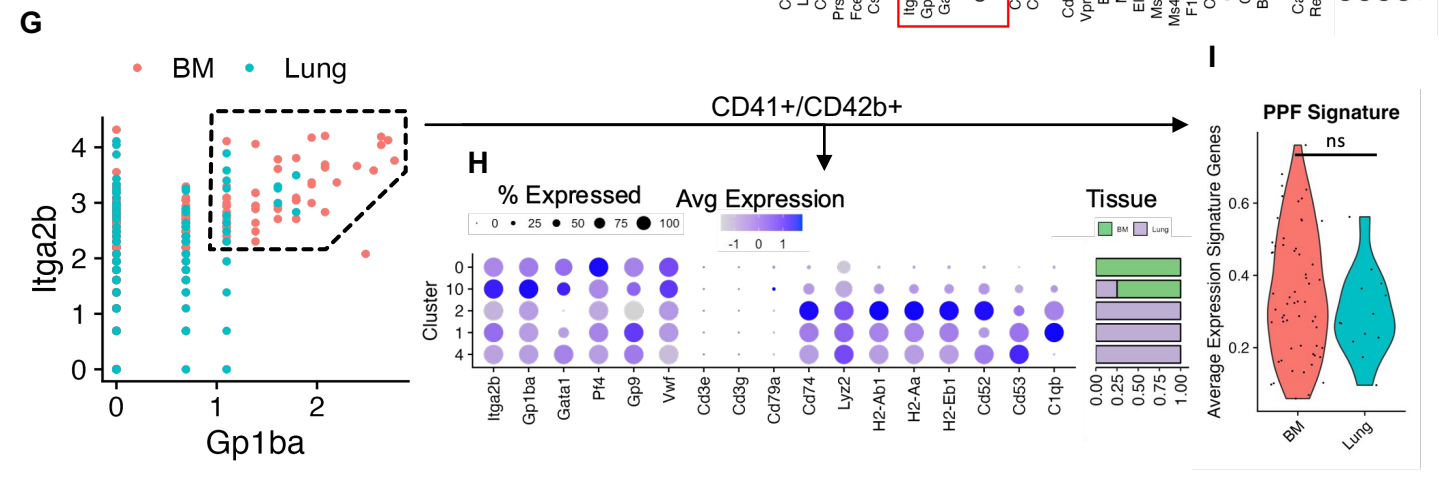
G
BM
Lung
Itga2b
Gp1ba
CD41+/CD42b+
H
% Expressed
0 25 50 75 100
Avg Expression
-1 0 1
Tissue
BM
Lung
Cluster
Itga2b Gp1ba Gata1 Pf4 Gp9 Vwf Cd3e Cd3g Cd79a Cd74 Lyz2 H2-Ab1 H2-Aa H2-Eb1 Cd52 Cd53 C1qb
0.00 0.25 0.50 0.75 1.00
I
PPF Signature
ns
Average Expression Signature Genes
BM
Lung

Figure 2

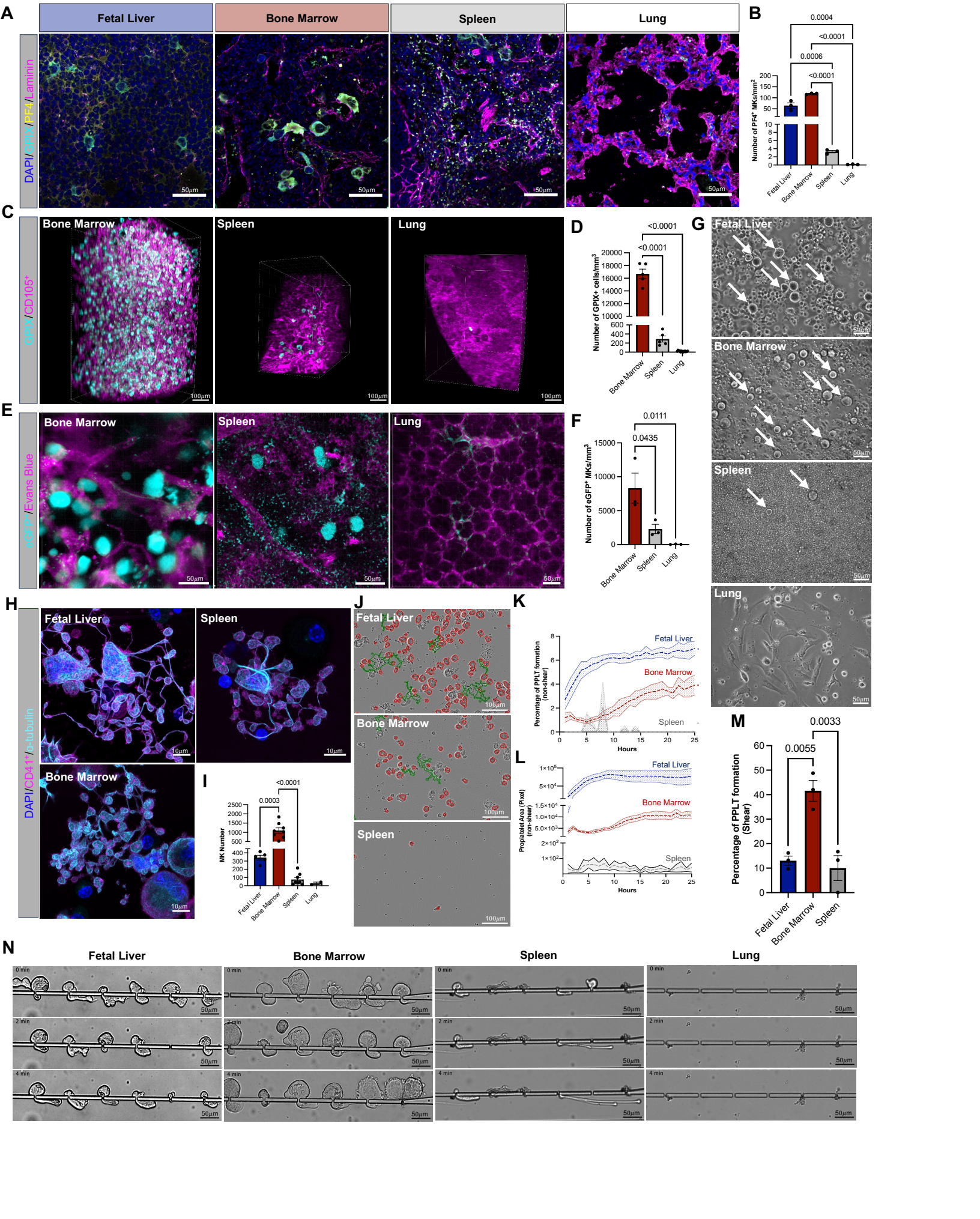
A
Fetal Liver
Bone Marrow
Spleen
Lung
DAPI/GPIX/PF4/Laminin
50μm
B
0.0004
<0.0001
0.0006
<0.0001
Number of PF4+ MKs/mm2
Fetal Liver
Bone Marrow
Spleen
Lung
C
Bone Marrow
Spleen
Lung
GPIX/CD105+
100μm
D
<0.0001
<0.0001
Number of GPIX+ cells/mm3
Bone Marrow
Spleen
Lung
E
Bone Marrow
Spleen
Lung
eGFP+/Evans Blue
50μm
F
0.0111
0.0435
Number of eGFP+ MKs/mm3
Bone Marrow
Spleen
Lung
G
Fetal Liver
Bone Marrow
Spleen
Lung
50μm
H
Fetal Liver
Spleen
Bone Marrow
DAPI/CD41+/b-tubulin
10μm
I
<0.0001
0.0003
MK Number
Fetal Liver
Bone Marrow
Spleen
Lung
J
Fetal Liver
Bone Marrow
Spleen
100μm
K
Fetal Liver
Bone Marrow
Spleen
Percentage of PPLT formation (non-shear)
Hours
L
Fetal Liver
Bone Marrow
Spleen
Propletelet Area (Pixel) (non-shear)
Hours
M
0.0033
0.0055
Percentage of PPLT formation (Shear)
Fetal Liver
Bone Marrow
Spleen
N
Fetal Liver
Bone Marrow
Spleen
Lung
0 min
2 min
4 min
50μm

The bone marrow is the primary site of thrombopoiesis

Nathan L. Asquith^[1,2], Estelle Carminita^[1,2], Virginia Camacho [1,2], Antonio Rodriguez-Romera [3], David Stegner [4,5], Daniela Freire [1], Isabelle C. Becker [1,2], Kellie R. Machlus [1,2], Abdullah Khan* [1,2,3,6], Joseph E. Italiano* [1,2]

1. Vascular Biology Program, Department of Surgery, Boston Children's Hospital, Boston, Massachusetts, United States.
2. Harvard Medical School, Boston, Massachusetts, USA.
3. MRC Weatherall Institute of Molecular Medicine, Radcliffe Department of Medicine, and National Institute of Health Research (NIHR) Oxford Biomedical Research Centre, University of Oxford, John Radcliffe Hospital/Headley Way, Oxford, United Kingdom.
4. Julius-Maximilians-Universität Würzburg, Rudolf Virchow Center for Integrative and Translational Bioimaging, Würzburg, Germany.
5. University Hospital Würzburg, Institute of Experimental Biomedicine, Würzburg, Germany.
6. Institute of Cardiovascular Sciences, College of Medical and Dental Sciences, University of Birmingham, Birmingham, United Kingdom.

*, ^, - *These authors have contributed equally.*

Text Word Count *1600*
Abstract Word Count *200*
Number of Figures *2*
Number of Supplementary Figures *4*

Corresponding Author: Dr. Joseph E. Italiano,
Joseph.italiano@childrens.harvard.edu
Karp Family Research Building
1 Blackfan Circle
Boston, MA 02215
617-919-5124

Data Sharing Statement: Please contact the corresponding author, Joseph Italiano, joseph.italiano@childrens.harvard.edu, for access to the original data related to this manuscript.

Key point:
In vitro. in vivo, and in silico data suggest that a small fraction of MKs reside in the lung and contribute minimally to the platelet pool

Abstract
Megakaryocytes generate thousands of platelets over their lifespan. More recently, roles in infection and inflammation have been reported. These findings have driven a study of extra-medullary thrombopoiesis, and megakaryocytes have been increasingly reported within the spleen and lung. However, the relative abundance of megakaryocytes in these organs compared to the bone marrow and the scale of their contribution to the platelet pool in steady state remains controversial. We investigated the relative abundance of megakaryocytes in the adult murine bone marrow, spleen, and lung using whole-mount light sheet and quantitative histological imaging, flow cytometry, intravital imaging, and an assessment of scRNA-seq repositories. Flow cytometry revealed significantly higher numbers of hematopoietic stem and progenitor cells and megakaryocytes in the murine bone marrow compared to spleens or perfused lungs. Two-photon intravital and light-sheet microscopy, as well as cryosections confirmed these findings. Moreover, ex-vivo cultured megakaryocytes from the bone marrow subject to static or microfluidic platelet production

assays had a higher capacity for proplatelet-formation than MKs from other organs. Analysis of previously published murine and human scRNA-seq datasets revealed that only a marginal fraction of megakaryocyte-like cells can be found within the lung and most likely only marginally contribute to platelet production in the steady state.

Introduction

Megakaryocytes (MKs) generate thousands of platelets, initially described as cells involved in hemostasis; however, researchers have identified a remarkable repertoire of functions of both cells in health and disease since these early reports. While platelets have elaborate roles in cancer metastasis, inflammation, and immunity, [1,2] MKs have been reported in several different organs, with roles beyond thrombopoiesis, such as the adaptive and innate immune responses. [3]

With their newfound attention, MKs have also become the subject of considerable controversy. Recent studies have reported that MKs in the lung contribute to 50% of platelet production in mice.[4] Conversely, human studies (albeit in patients with cardiac abnormalities) estimated that intravascular MKs in the lung contributed 7-17% of all platelets.[5] Lung MKs have been reported to be of low ploidy and demonstrate immune-like transcriptional profiles. [6,7] A similar subpopulation of bone marrow resident $LSP1^+/CD53^+$ MKs has been associated with pathogen recognition and clearance. [8] Splenic MKs, on the other hand, are a significant source of platelet production upon inflammatory challenges such as sepsis. [9] With increasing, contradicting reports of extramedullary MKs and their contribution to physiological platelet production, there is a pressing need for a consensus on their definition, role, and relative abundance in healthy tissues and are reports of MKs in these tissues confounded by what we define as a MK.

Methods

For full methods, please refer to supplementary material.

Organs

Bones (Femurs, tibias, iliac crests), spleens, and lungs were harvested from C57BL/6J mice. Mouse fetal livers were harvested from CD-1 mice.

Flow cytometry

Single-cell suspensions were analyzed by flow cytometry; total numbers of long-term hematopoietic stem cells (LT-HSCs), MK progenitors (MkPs), and MKs were quantified for all organs.

In-situ quantification of MK numbers

Immunofluorescence microscopy was performed on cryosections labeled with MK markers MK number/mm^2 was calculated for all organs.

Light-sheet fluorescence microscopy (LSFM)

Organs from C57BL/6JRj mice were perfusion-fixed, chemically cleared using BABB, and imaged by light-sheet fluorescence microscopy as described previously. [10] MK number/mm^3 was calculated.

Two-photon intravital microscopy (2PIVM)

Intravital videos of each organ within C57BL/6JR (vWF-eGFP) mice were obtained, and MKs ($eGFP^+$) and vessels (Evans Blue) were visualized using a 960nm laser line. MK number/mm^3 was calculated.

Ex-vivo quantification of MK numbers

HSPCs were expanded and supplemented with thrombopoietin (TPO). MKs were enriched by a density gradient and imaged. The total number of MKs per culture was calculated.

In vitro proplatelet formation assay

MKs cultured from ex-vivo HSPCs were imaged for 24 hours. Pixel-based machine learning distinguished MKs from proplatelets, and proplatelet-making capacity was quantified.

Shear-driven proplatelet formation assay

MKs cultured from HSPCs were infused into a microfluidic device and formed proplatelets in the flow direction; widefield phase images of proplatelet formation were acquired. Percentage proplatelet formation was calculated for each organ.

Bioinformatic analysis

Single-cell (sc)RNA-seq and CITE-seq datasets were analyzed using R, RStudio, and Seurat. scRNAseq count matrices from murine bone marrow and lung were obtained from the online repository GEO (accession: GSE152574) and processed using the authors' parameters. Principal Component Analysis (PCA) was performed, and the top 20 principal components were used to compute the unsupervised Uniform Manifold Approximation and Projection (UMAP) and the clusters. Seurat objects for human lung and bone marrow single cell atlases were obtained from the following repositories: Lung, BoneMarrow. Data were imported to R and visualized using Seurat and ggplot2. MKs were identified using the metadata provided on the objects.

Results and Discussion

We quantified the total number of hematopoietic stem and progenitor cells (HSPCs) as well as MKs in freshly isolated murine fetal livers (*n* = 3), adult spleens, lungs, and bone marrow (*n* = 5) **(Figure 1A)**. To indicate whether MKs were tissue-resident or derived from alternative sources, the number of LT-HSCs ($CD45^+Lin^-Sca1^+CD48^-CD150^+$) was quantified for each tissue. In adult tissues, LT-HSCs were most abundant in bone marrow, with 11.8-fold (±7.3) and 75.4-fold (±43.9) more cells than in the spleen and lung **(Figure 1B).** Most LT-HSCs were found in the mouse fetal liver (0.7-fold higher than bone marrow). MKPs ($CD45^+Lin^-Sca1^+CD41^+CD150^+$) were primarily found in the bone marrow, with a 7.1-fold and 45.7-fold increase in cells compared to spleen and lung **(Figure 1C**), while murine fetal livers displayed a 19.2-fold decrease compared to the bone marrow.

Similarly, the total number of mature MKs ($CD45^+Lin^-CD41^+CD42d^+$) was highest within the bone marrow and significantly lower in the spleen (-2.6 fold ± 1.1) and lung (-11.2 fold ± 6.2) and comparatively lower in the fetal liver (-8.5 fold ± 3.2) **(Figure 1D)**. The negligible number of LT-HSC and MKPs in the lung suggests that this tissue is not a significant site for megakaryopoiesis and implies that MKs previously identified in this tissue have an extra-pulmonary source.

We investigated murine scRNA sequencing datasets on $CD41hi^+$ cells isolated from bone marrow or lung to categorize MKs or MK-like cells from these tissues transcriptionally.[6] CD41 is widely used as a MK marker (alone or in conjunction with CD42); however, our data revealed that only a subset of $CD41^+$ cells were positive for canonical MK genes (*Itga2b, Gp1ba, Gata1, Pf4, Gp9, Vwf*), with the remaining cells expressing progenitor- and immune-cell-like (Eo/Baso/Mast) genes **(Figure 1E, F)**. We subsetted the MKs based on Cd41 (Itga2b) and Cd42b (Gp1ba) expression **(Figure 1G)** and found 42/2040, ~ 2% cells from the lung to classify as megakaryocytic, while the majority of bone marrow-derived cells did classify (626/668 ~ 94%). In line with previous studies [6], we found a fraction of pulmonary $CD41^+CD42b^+$ cells to express immune genes **(Figure 1H, 1I),** and no niche MKs were detected in the lung (**Supplementary Figure 1**). We next assessed previously published scRNAseq atlases of the human lung, [11], which identified only a marginal number of the cells as MKs (11/60993 ~0.02%) **(Supplementary Figure 2)**. However, an analysis of RNA expression shows that none of these cells (or any of the other cell types identified in the human lung) express canonical MK markers. Our previous data suggest that CD41 might be insufficient in identifying a pure MK subset. Using CITE-seq atlas (single-cell RNA + antibody-based cell surface protein expression), [12], we found CD41 highly expressed on MKs and other myeloid cells **(Supplementary Figure 2C, 2D)**. This data points to a need for a consensus concerning the isolation, identification, and characterization of MKs.

We next performed in situ fluorescence labeling of cryosections with antibodies against canonical MK markers CD41 **(Supplementary Figure 3)**, GPIX, and PF4 **(Figure 2A, Supplementary Figure 3)**. Quantitative analysis of MK numbers **(Figure 2B, Supplementary Figure 3)** revealed that the fetal liver and bone marrow displayed the highest number of MKs. Few MKs were observed in the spleen, consistent with previous data reporting that splenic thrombopoiesis is inflammation-driven.[9]

In contrast to recent studies, we only observed a marginal number of MKs in cryosections derived from perfused lungs. To support our in-situ labeling data, we also performed LSFM quantifying events positive for GPIX and >16 µm in diameter **(Figure 2C, 2D)**. Additionally, using vWF-eGFP reporter mice, we also performed intravital imaging to quantify events **(Figure 2E, 2F).** Using both methods, we observed that MK numbers were significantly higher in bone marrow compared to spleen or lung. While we very rarely observed intravascular MKs passing through the lung vasculature, no extravascular events were observed **(Supplementary Figure 4).** These findings strongly support our ex vivo data and highlight that the bone marrow is the primary site of megakaryo- and thrombopoiesis.

Due to the difficulty of isolating native MKs for proplatelet formation assays, we cultured and expanded progenitors from each organ, differentiated them into MKs using TPO, and isolated the resulting MKs by size exclusion enrichment **(Figure 2G)**. When quantifying the total number of MKs ($CD41^+$ and >20 µm), all tissues except the lung exhibited proplatelet-forming MKs **(Figure 2H, I)**. The number of cells was highest in fetal liver and bone marrow, followed by spleen and lung. We hypothesize that low numbers of LT-HSCs and MKPs in the lung (as supported by our flow cytometry data) make it challenging to differentiate HSPCs to MKs in this organ in vitro.

Shear forces have been reported to be critical for proplatelet formation.[13] We assessed proplatelet formation of MKs cultured ex vivo from HSPCs under non-shear **(Figure 2J, - 2L)** and shear conditions **(Figure 2M, 2N).** Due to the negligible amount of HSPCs in the lung, it was impossible to quantify the capacity for proplatelet formation of lung-derived cells. Quantification of fetal liver and bone marrow-derived MKs revealed that shear increased proplatelet formation from cultured fetal liver-derived MKs by 90%, consistent with our previous findings.[13] In comparison, shear increased proplatelet formation from cultured bone marrow-derived MKs by ~1000%, highlighting the importance of sinusoidal shear for proplatelet formation.

Our data revealed high LT-HSC, MKP, and MK numbers in the bone marrow compared to the spleen or lung by flow cytometry, which was supported by in situ fluorescence, LSFM, and intravital imaging, thus demonstrating that the spleen and lung are not critical sites of megakaryopoiesis in adult mice upon steady state. Thus, assuming they marginally contribute to the overall platelet pool is reasonable. Analysis of published murine and human scRNA-seq datasets supports the observation that only a marginal fraction of MKs is found within the lung. Intriguingly, this analysis also revealed that only a subset of $CD41^+$ cells classify as MKs in the lung based on their expression of canonical MK genes. The variety of recent work highlighting the non-conventional roles of MKs makes it necessary to find clear criteria for defining MKs based on their transcriptional profile, surface marker expression, and morphology. Our work is a first step to finding a more precise definition of which MKs contribute to platelet production.

References

1. Lucotti S, Muschel RJ. Platelets and Metastasis: New implications of an old interplay. *Frontiers in Oncology.* 2020;10.
2. Portier I, Campbell RA. Role of platelets in detection and regulation of infection. *Arteriosclerosis, Thrombosis, and Vascular Biology.* 2021;41(1):70-78.
3. Semple JW, Italiano JE, Freedman J. Platelets and the immune continuum. *Nature Reviews Immunology.* 2011;11(4):264-274.
4. Lefrançais E, Ortiz-Muñoz G, Caudrillier A, et al. The lung is a site of platelet biogenesis and a reservoir for haematopoietic progenitors. *Nature.* 2017;544(7648):105-109.
5. Kaufman RM, Airo R, Pollack S, Crosby WH. Circulating megakaryocytes and platelet release in the Lung. *Blood.* 1965;26(6):720-731.
6. Yeung AK, Villacorta-Martin C, Hon S, Rock JR, Murphy GJ. Lung megakaryocytes display distinct transcriptional and phenotypic properties. *Blood Advances.* 2020;4(24):6204-6217.
7. Pariser DN, Hilt ZT, Ture SK, et al. Lung megakaryocytes are immune modulatory cells. *J Clin Invest.* 2021;131(1).
8. Sun S, Jin C, Si J, et al. Single-cell analysis of ploidy and the transcriptome reveals functional and spatial divergency in murine megakaryopoiesis. *Blood.* 2021;138(14):1211-1224.
9. Valet C, Magnen M, Qiu L, et al. Sepsis promotes splenic production of a protective platelet pool with high CD40 ligand expression. *J Clin Invest.* 2022;132(7).
10. Stegner D, vanEeuwijk JMM, Angay O, et al. Thrombopoiesis is spatially regulated by the bone marrow vasculature. *Nature Communications.* 2017;8(1):127.
11. Travaglini KJ, Nabhan AN, Penland L, et al. A molecular cell atlas of the human lung from single-cell RNA sequencing. *Nature.* 2020;587(7835):619-625.
12. Triana S, Vonficht D, Jopp-Saile L, et al. Single-cell proteo-genomic reference maps of the hematopoietic system enable the purification and massive profiling of precisely defined cell states. *Nat Immunol.* 2021;22(12):1577-1589.
13. Thon JN, Mazutis L, Wu S, et al. Platelet bioreactor-on-a-chip. *Blood.* 2014;124(12):1857-1867.

Acknowledgments

We thank Emma Nikols, Clementine Payne, and Karen Guo for excellent technical support. We want to thank Calixto Saenz and the Harvard Microfluidic Core for fabricating the microfluidic devices used in this study. We thank Maximilian Voll (née Gorelashvili) for help with the LSFM image acquisition and the Core Unit Fluorescence Imaging of the Rudolf Virchow Center for help with LSFM data acquisition and analysis. We thank Pierre Cunin and Peter Nigrovic (Boston Children's Hospital) for assistance with 2PIVM. We also thank Carla Asquith for her intellectual discussions and critical manuscript review.

N.L.A., E.C., D.F., and J.E.I. are supported by the National Institute of Health, National Heart, Lung, and Blood Institute (R01HL68130 and R35HL161175). A.R.R. is supported by the Medical Research Council, United Kingdom (H4R02651). V.C. is supported by the NIH National Research Service Award (NRSA) Fellowship (5T32HL007917-22). D.S is supported by the German Research Foundation (#374031971 - CRC1525). I.C.B. is supported by a Walter Benjamin Fellowship of the German Research Foundation (BE 7766/2-1). KRM is supported by the National Institute of Diabetes and Digestive and Kidney Diseases

(R03DK124746) and the National Heart, Lung, and Blood Institute (R01HL151494). A.O.K is a Sir Henry Wellcome Fellow supported by the Wellcome Trust (218649/A/19/Z).

Authorship Contributions

Contribution: N.L.A conducted experiments, analyzed and interpreted the data, and wrote the manuscript; E.C., V.C., D.S., A.A.R., D.F., and I.B. designed and performed experiments and analyzed and interpreted the data. I.C.B. and K.R.M. critically reviewed the manuscript. A.K. and J.E.I. conceptualized and designed the research and critically reviewed the manuscript.

Disclosure of Conflicts of Interest

Conflict-of-interest disclosure: J.E.I. has a financial interest in and is a founder of StellularBio, a biotechnology company focused on making donor-independent platelet-like cells at scale. Boston Children's Hospital manages the interests of J.E.I. All other authors declare no competing financial interests.

Figure Legends

Figure 1. Ex-vivo profiling of megakaryocytes by flow cytometry and single-cell RNA-seq demonstrates that the bone marrow is the leading site of megakaryopoiesis in mice. (A) Representative dot plots of HSPC cells, MKPs, and MKs. (B) Absolute long-term HSC (LT-HSC) cell counts across tissues: bone marrow, spleen, and lung n = 5 animals, fetal liver n = 3 animals. (C) Absolute counts of MkP cells across tissues: bone marrow, spleen, and lung n = 5 animals, fetal liver n = 3 animals. (D) Absolute counts of MK cells across tissues: bone marrow, spleen, and lung n = 5 animals, fetal liver n = 3 animals. Blue = fetal liver, red = bone marrow, grey = spleen, and white = lung. Data are shown as mean ± SEM. Statistics were performed with 1-way ANOVA with Tukey's multiple comparisons test at 95% CI: *P < 0.05, **P < 0.01, ***P < 0.001, ****P < 0.0001. (E) UMAP projection of scRNAseq datasets (of murine lung and bone marrow $CD41^+$ cells (Yeung Blood Advances, 2020). Plots are colored by sampling tissue (left) or cluster identity (right). (F) Bubble plot showing expression of common murine hematopoiesis markers across clusters. The red box highlights canonical MK markers. (G) Scatter plot showing gating strategy used to select $CD41^+CD42^+$ cells based on RNA expression. (H) Bubble plot showing MK and immune-related markers expression on $CD41^+CD42^+$ cells across clusters. (I) Average expression of genes from a Pro-Platelet Formation (PPF) signature on $CD41^+CD42^+$ cells.

Figure 2. In situ, fluorescence labeling, light-sheet fluorescence (LSFM), 2PIVM, and ex vivo proplatelet assays demonstrate that the bone marrow is the primary site of megakaryocytes in adult mice. (A) Structured illumination micrographs of cryosections obtained from mouse fetal liver, bone marrow, spleen, and lung, respectively. Blue = DAPI, cyan = GPIX, yellow = PF4, magenta = laminin. Scale bars are 50 μm. (B) Quantitative analysis of megakaryocyte count within whole organ cryosections (PF4) MK/mm^2, blue = fetal liver, red = bone marrow, grey = spleen, and white = lung. (C) Reconstruction of LSFM data of femoral bone marrow, spleen, and lung tissues. MKs are depicted in cyan (anti-GPIX) and vessels in magenta (anti-CD105); scale 100 μm. (D) Quantification of MK ($GPIX^+$, >16μm) numbers per mm^3 in the adult mouse bone marrow, spleen, and lung; bar graphs represent mean ± SD. Red = bone marrow, grey = spleen, and white = lung. (E) Representative images of 2PIVM data of adult mouse bone marrow, spleen, and lung tissues. MKs ($eGFP^+$, >16μm) are depicted in cyan and vessels in magenta (Evans Blue, Scales bars represent 50μm. (F) Quantification of 2PIVM data shows an average number of MKs per mouse. Red = bone marrow, grey = spleen, and white = lung. (G) Representative brightfield images of day four mouse fetal liver, bone marrow, spleen, and lung cultures pre-gradient. White arrows indicate megakaryocytes. Scale bars are 50μm. (H) Representative, structured illumination micrographs of proplatelet-forming megakaryocytes differentiated ex vivo from mouse fetal liver, bone marrow, and spleen progenitors. Blue = DAPI, magenta = $CD41^+$, cyan = α-tubulin. Scale bars represent 10μm. (I) Quantitative analysis of megakaryocyte counts on day four megakaryocytes differentiated ex vivo, blue = fetal liver, red = bone marrow, grey = spleen, and white = lung. (J) Representative phase contrast images of proplatelet forming megakaryocytes from multiple tissues at 24 h time points. Red = megakaryocytes, green = proplatelet extensions. Scale bars represent 100μm. (K) Quantitative analysis of the percentage of megakaryocytes forming proplatelets blue = fetal liver, red = bone marrow, grey = spleen. (L) Total proplatelet area of MKs forming proplatelets blue = fetal liver, red = bone marrow, grey = spleen. (M) Percentage of megakaryocytes forming proplatelets in shear conditions. Blue = fetal liver, red = bone marrow, grey = spleen. (N) Representative panels of shear-driven proplatelet formation and extension in a microfluidic device over time for ex vivo differentiated MKs from multiple tissues. The time scale is T = 0 min → 4 min. Scale bars represent 50μm. Unless otherwise stated, all data sets are shown as mean ± SEM; graphs represent data from a minimum of 3 independent mice. Statistics were performed with 1-way ANOVA with Tukey's multiple comparisons test at 95% CI: *P < 0.05, **P < 0.01, ***P < 0.001, ****P < 0.0001.